Bulletin of Electrical Engineering and Informatics
Vol. 10, No. 3, June 2021, pp. 1739~1746
ISSN: 2302-9285, DOI: 10.11591/eei.v10i3.2262

A compact dual-band semi-flexible antenna at 2.45 GHz and 5.8 GHz for wearable applications

S. M. Shah[1], A. A. Rosman[2], M. A. Z. A. Rashid[3], Z. Z. Abidin[4], F. C. Seman[5], H. A. Majid[6], S. H. Dahlan[7], S. A. Hamzah[8], N. Katiran[9], A. Ponniran[10], F. Hassan[11], F. Zubir[12]
[1,4,5,6,7,8]Research Center for Applied Electromagnetics, Universiti Tun Hussein Onn Malaysia, 86400 Batu Pahat, Johor
[2,3,9,10]Faculty of Electrical and Electronic Engineering, Universiti Tun Hussein Onn Malaysia, 86400 Batu Pahat, Johor
[11,12]School of Electrical Engineering, Faculty of Engineering, Universiti Teknologi Malaysia, 81310 Johor Bahru, Johor

Article Info

Article history:

Received Sep 29, 2020
Revised Feb 17, 2021
Accepted Mar 25, 2021

Keywords:

Bending investigation
Dual-band antenna
ISM band
Specific absorption rate
Wearable antenna

ABSTRACT

In this work, a compact dual-band semi-flexible antenna operating at 2.45 GHz and 5.8 GHz for the industrial, scientific and medical (ISM) band is presented. The antenna is fabricated on a semi-flexible substrate material, Rogers Duroid RO3003™ with a low-profile feature with dimensions of 30×38 mm^2 which makes it a good solution for wearable applications. Bending investigation is also performed over a vacuum cylinder and the diameters are varied at 50 mm, 80 mm and 100 mm, that represents the average human arm's diameter. The bending investigation shows that reflection coefficients for all diameters are almost similar which imply that the antenna will operate at the dual-band resonant frequencies, even in bending condition. The simulated specific absorption rate (SAR) in CST MWS® software shows that the antenna obeys the FCC and ICNIRP guidelines for 1 mW of input power. The SAR limits at 2.45 GHz for 1 g of human tissue is simulated at 0.271 W/kg (FCC standard: 1.6 W/kg) while for 10 g is at 0.0551 W/kg (ICNIRP standard: 2 W/kg. On the other hand, the SAR limits at 5.8 GHz are computed at 0.202 W/kg for 1 g and 0.0532 W/kg for 10 g.

Corresponding Author:

Shaharil Mohd Shah
Research Center for Applied Electromagnetics (EMCenter)
Universiti Tun Hussein Onn Malaysia
86400 Batu Pahat, Johor, Malaysia
Email: shaharil@uthm.edu.my

1. INTRODUCTION

These days, microstrip antennas are prevalent because of their low profile, light weight, flexibility and compatibility with integrated circuits [1]-[3]. Multiband microstrip antennas are required in various applications such as the wireless local area network (WLAN), wireless interoperability microwave access (WiMAX) and long term evolution (LTE) [4], [5]. Generally, the term dual-band antenna refers to two significant frequencies that the antenna can operate. This can be achieved by combining two frequency bands in the antenna design. One popular method to generate a dual-band frequency of operation is by introducing a slot on the radiating patch so as to alter the current path which governs the formation of each resonant frequency [6], [7].

Wearable antennas are essentially any antennas that are specifically designed to function while being worn on-body [8]. This requires the antenna to be very compact with a certain degree of flexibility, so as not to cause discomfort to the user. Due to the flexibility and durability of wearable antennas, they have been used in a widespread range of applications known as objects observation, wireless medical purposes and

wireless communications, just to name a few [9]-[11]. Specific absorption rate (SAR) is described as a degree of rate at which energy is absorbed by the body when exposed to an electromagnetic field from an antenna [12], [13]. The European Union (EU) SAR limit is 2 W/kg averaged over 10 g of tissue following the IEC standard for wireless device (IEC 62209-1) [14]. On the other hand, the Federal Communication Commission (FCC) requires that the SAR should be lower than 1.6 W/kg averaged over 1 g tissues in the United States [15]. Influence of body proximity on the performance of antenna and the amount of SAR absorbed by human body are the two significant on-body requirements for wearable antennas.

The industrial, scientific and medical (ISM) frequency bands are reserved for international purpose in the non-commercial applications of industrial, scientific and medical applications [16]. The ISM bands are license-free with low power consumption [17]. Therefore, multiple work have been performed for the integration of ISM bands in a single device [18], [19]. The 2.45 GHz ISM band is a widely accepted frequency band for worldwide operations [20].

Traditional antennas are known to be rigid and inflexible, which makes them not a popular choice for wearable applications [21], [22]. On the contrary, wearable antennas are required to be flexible as they need to follow the body curves and bent for the comfort of the users. In addition, wearable antennas must be small and light weight as they are designed to be incorporated into clothings [23]. Hence, a semi-flexible wearable antenna (due to the nature of Rogers Duroid RO3003™ substrate material used in this work) for wearable applications is presented in this work as it offers the solutions for both rigidity and inflexibility of traditional antennas [24]. The dimensions of the antenna is designed to be compact so as not to cause discomfort to the user when being worn on body while at the same time, offers good flexibility. The proposed antenna will operate dual-band at 2.45 GHz and 5.8 GHz of the ISM bands for WLAN application in both the lower and upper frequency bands. This advantage will serve as an added-value to the proposed antenna.

2. RESEARCH METHODOLOGY

2.1. Antenna design and configuration

The design and simulation of the antenna are performed by using CST MWS® software. Optimization has been performed in obtaining the exact dimensions to achieve the required frequency at 2.45 GHz and 5.8 GHz of the ISM bands with the best linear characteristics. A modified ground plane with dimensions of $W_{pg} \times L_{pg}$ mm^2 has been introduced in this design to further improve the reflection coefficient and an L-shaped slot is used to generate the upper frequency band of the antenna. Figure 1 shows the geometry of the proposed dual-band semi-flexible wearable antenna at 2.45 GHz and 5.8 GHz while Table 1 lists the dimensions of the antenna.

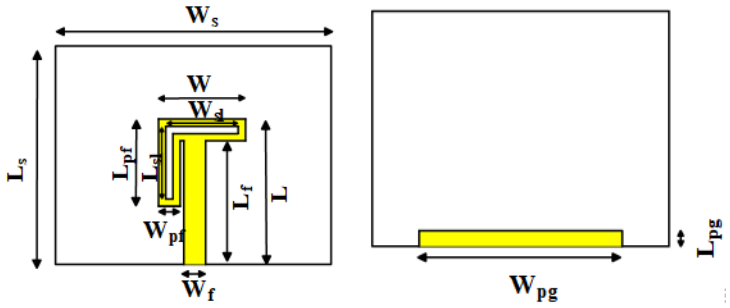

(a) (b)

Figure 1. The proposed dual-band semi-flexible antenna at 2.45 GHz and 5.8 GHz, (a) Top view, (b) Bottom view

Table 1. Dimensions of the dual-band semi-flexible antenna

Parameters	Values (mm)	Parameters	Values (mm)
L	20	W_{pf}	3
W	12	L_{sl}	10
Ls	30	W_{sl}	10
W_S	38	L_{pg}	2
L_f	17	W_{pg}	26
W_f	3	h_t	0.035
L_{pf}	12	h_S	1.52

2.2. Antenna simulation in bending condition

The bending investigation is performed and simulated in CST MWS® software along the y-axis over a vacuum cylinder with diameters, d are varied at 50 mm, 80 mm and 100 mm to approximate the average human arm's diameter.

2.3. Antenna simulation of specific absorption rate

Since the dual-band wearable antenna will be used on human body, a numerical human phantom model has been replicated in CST MWS® software to investigate the performance of the antenna while operating within a close proximity to the human body in terms of the specific absorption rate (SAR). In order to develop the numerical human phantom design, the information on the each layer of human tissue such as the dielectric constant, density and conductivity at the operating frequency of 2.45 GHz and 5.8 GHz are necessary [25] and has been included in the simulations. The antenna is placed at 2 mm over the human phantom model to take into account the approximate thickness of the clothings worn by the user.

2.4. Antenna fabrication and measurement

The prototypes of the dual-band wearable antenna can be viewed in Figure 2. The antenna is fabricated on a semi-flexible substrate material, Rogers Duroid RO3003™ with the following properties: relative permittivity, ε_r of 3, loss tangent, tan δ of 0.0010 and thickness, h of 1.52 mm. The ZVB14 Rohde & Schwarz Vector Network Analyser is used to measure the antenna.

(a) (b)

Figure 2. The fabricated dual-band semi-flexible antenna at 2.45 GHz and 5.8 GHz, (a) Top view, (b) Bottom view

3. RESULTS AND ANALYSIS

3.1. Reflection coefficient on a flat surface

Figure 3 shows the comparison of simulated and measured reflection coefficients of the dual-band semi-flexible wearable antenna at 2.45 GHz and 5.8 GHz. From the figure, the proposed antenna operates at 2.45 GHz with a simulated reflection coefficient, S_{11} of -13.472 dB and 5.8 GHz with S_{11} of -19.516 dB. The resonant frequencies of the fabricated antenna are measured at 2.65 GHz and 5.83 GHz with S_{11} of -32.37 dB and -32.05 dB, respectively. The shift of the measured resonant frequencies with respect to the simulated can be attributed to the fabrication tolerances and cable losses. However, the measured S_{11} when the marker is placed at 2.45 GHz and 5.8 GHz are -11.741 dB and -18.587 dB, respectively which show that the antenna can still operate at the desired ISM frequency bands of 2.45 GHz and 5.8 GHz.

3.2. Radiation pattern

The radiation patterns of the dual-band wearable antenna have been simulated at 2.45 GHz and 5.8 GHz. Figure 4 shows the radiations patterns of the antenna in the *E*-plane and *H*-plane at 2.45 GHz while Figure 5 illustrates the radiations patterns of the antenna at 5.8 GHz in both planes. From the figure, it can be observed that the radiation patterns at the lower resonant frequency of 2.45 GHz is almost bi-directional in the *E*-plane and omnidirectional in the *H*-plane. The bi-directional radiation pattern in the *E*-plane deteriorates at 5.8 GHz while the omnidirectional pattern remains in the *H*-plane.

3.3. Surface current distribution

Figure 6 shows the surface current distribution of the antenna at 2.45 GHz and 5.8 GHz. It can be seen from the figure that the maximum surface current is concentrated around the edges of the microstrip feedline at 2.45 GHz. On the other hand, the maximum surface current is seen to be dominant around the edges of the slot at 5.8 GHz. The observation is consistent with the theoretical explanation from the literature

that the length of the current path travels on the radiating patch does affect the resonant frequency [26]. The longer the current path travels across the radiating patch, the lower the resonant frequency or vice versa. Thus, as can be seen in the figure, the current path represented by the maximum current distribution is longer at the lower frequency which contributes to the lower resonant frequency at 2.45 GHz. On the other hand, the opposite occurs which is responsible to the formation of higher resonant frequency at 5.8 GHz.

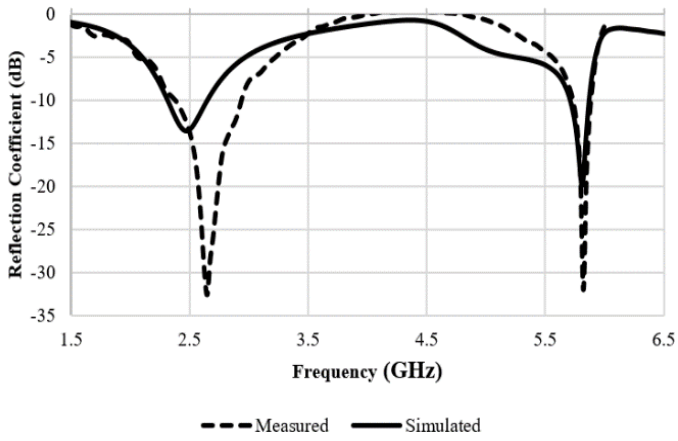

Figure 3. The comparison of simulated and measured reflection coefficients of the dual-band semi-flexible antenna

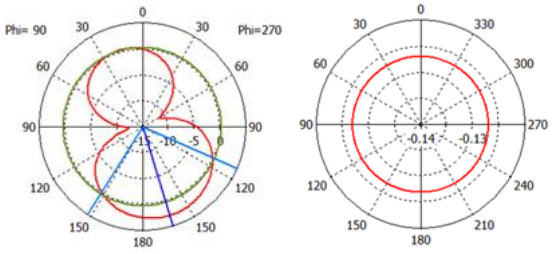

(a) (b)

Figure 4. Radiation patterns of the dual-band semi-flexible antenna at 2.45 GHz in the, (a) *E*-plane, (b) *H*-plane

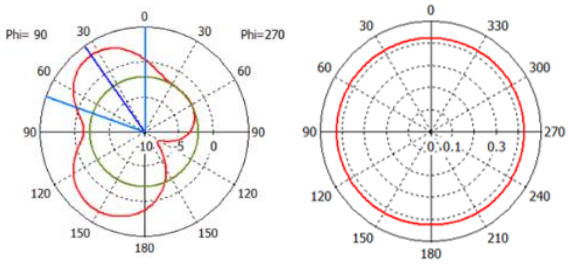

(a) (b)

Figure 5. Radiation patterns of the dual-band semi-flexible antenna at 5.8 GHz in the, (a) *E*-plane, (b) *H*-plane

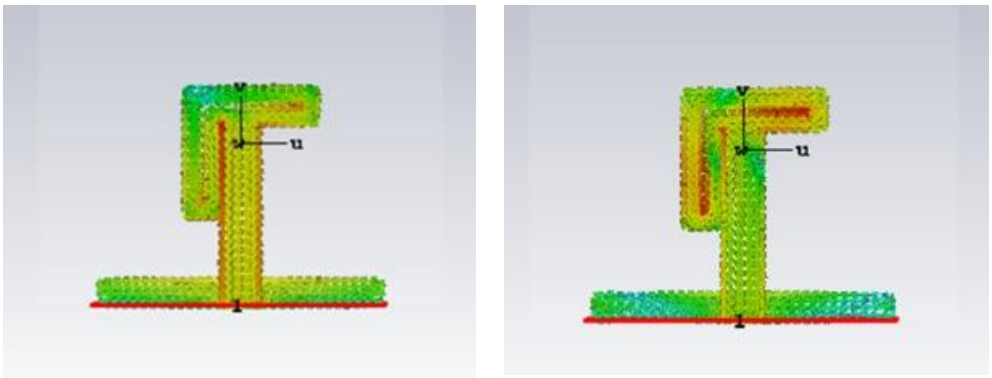

(a) (b)

Figure 6. Surface current distribution of the dual-band semi-flexible antenna at, (a) 2.45 GHz, (b) 5.8 GHz

3.4. Bending investigation

Figure 7 shows the simulated reflection coefficients, S_{11} of the antenna in bending condition with varying approximate diameter, *d* of human arms with *d*=50 mm, 80 mm and 100 mm along the *y*-axis in CST MWS® software. From the figure, it can be observed that the reflection coeffitients for all diameters are very similar with a very slight difference to be seen in the upper frequency band for *d*=50 mm. In this case, the upper resonant frequency is shifted to 5.75 GHz with S_{11} of -25 dB. Nevertheless, the S_{11} when the marker is placed at 5.8 GHz is still acceptable at -13.23 dB which implies that the antenna can still operate at the upper resonant frequency of 5.8 GHz. The results show that the wearable antenna is working well under bending condition regardless of the approximate diameter of human arms.

Figure 8 shows the measured S_{11} of the antenna over varying diameter of PVC pipes to emulate the human arms. From the figure, a shift in the resonant frequency is observed for each diameter. The differences between the simulation and measurement results might be attributed to antenna's misalignment. Table 2 lists the comparison between the simulated and measured S_{11} in bending condition. As can be viewed from the table, the simulation and measurement results of the antenna fairly agree with each other in bending condition.

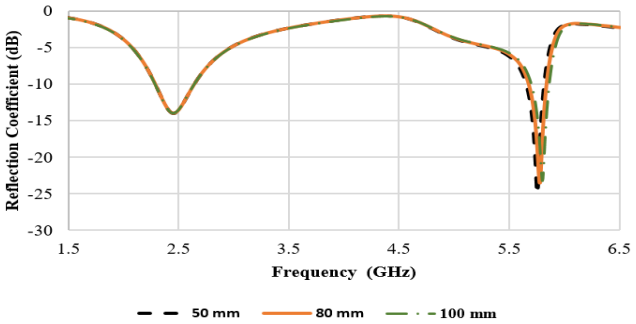

Figure 7. The simulated reflection coefficients of the dual-band semi-flexible antenna in bending condition over varying diameter, *d* of human arms in CST MWS® software when *d* is, (a) 50 mm, (b) 80 mm, (c) 100 mm

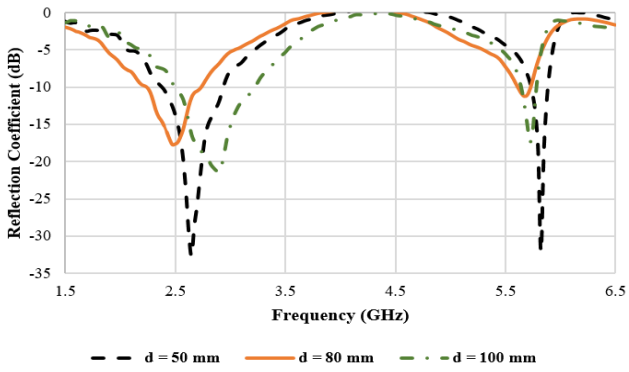

Figure 8. The measured reflection coefficients of the dual-band semi-flexible antenna in bending condition over varying diameter, *d* of PVC pipes to emulate human arms when *d* is, (a) 50 mm, (b) 80 mm, (c) 100 mm

Table 2. Comparison between the simulated and measured S_{11} of the dual-band semi-flexible antenna in bending condition

Diameter, d (mm)	Simulated Resonant Frequency (GHz)	Measured Resonant Frequency (GHz)
50	2.45 & 5.8	2.60 & 5.83
80	2.45 & 5.8	2.51 & 5.71
100	2.45 & 5.8	2.90 & 5.73

3.5. Specific absorption rate

Figures 9 and 10 show the simulated SAR values of the antenna at 2 mm away from the numerical human phantom model for 1 mW input power. The 2 mm distance is chosen as the approximate thickness of fabric materials worn by human as the antenna will not be placed directly on the bareskin but instead on the

clothing of the user. From the figure, it is observed that at 2.45 GHz, the SAR limits of the antenna are simulated at 0.271 W/kg for 1 g and 0.0551 W/kg for 10 g. On the other hand, the SAR limits at 5.8 GHz are computed at 0.202 W/kg for 1 g and 0.0532 W/kg for 10 g. Therefore, 1 mW of input power is used for this work because it obeys the FCC and ICNIRP guidelines.

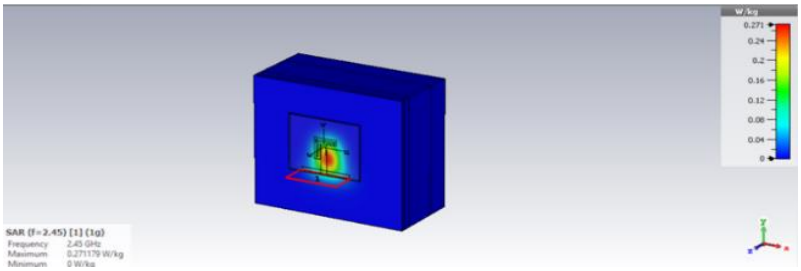

(a)

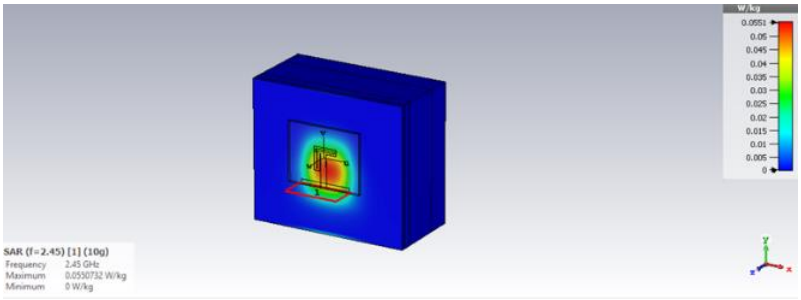

(b)

Figure 9. The simulated SAR values of the dual-band semi-flexible antenna placed at 2 mm away from the numerical human phantom model for 1 mW input power at 2.45 GHz with tissue weight of, (a) 1 g, (b) 10 g

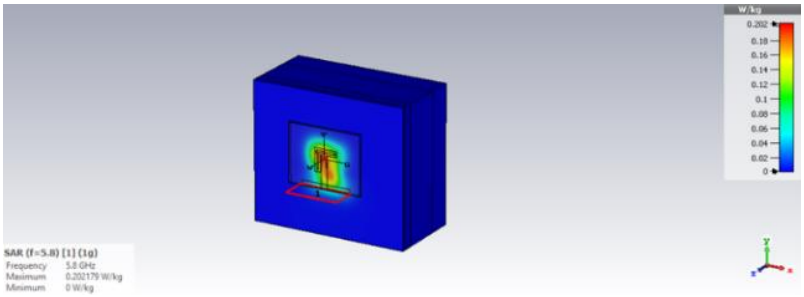

(a)

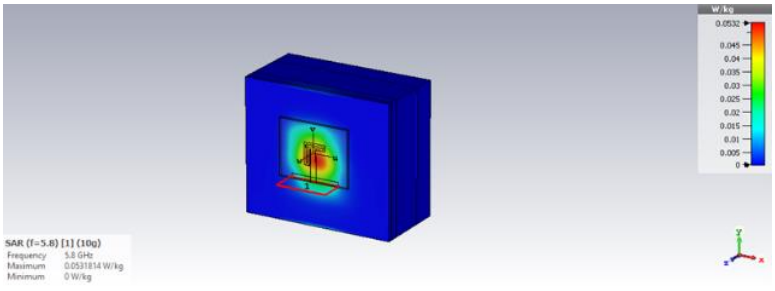

(b)

Figure 10. The simulated SAR values of the dual-band semi-flexible antenna placed at 2 mm away from the numerical human phantom model for 1 mW input power at 5.8 GHz with tissue weight of, (a) 1 g, (b) 10 g

4. CONCLUSION

A dual-band semi-flexible microstrip antenna with Rogers Duroid RO3003™ substrate at 2.45 GHz and 5.8 GHz of the license-free ISM bands is presented in this work. The antenna is designed to be compact with dimensions of 30 × 38 mm^2 to avoid discomfort to the user when the antenna is worn on body and offers good flexibility, at the same time. The antenna bending performance on the approximate human arm diameters is also investigated to evaluate the performance of the antenna for wearable applications. The simulation and measurement results show that the antenna is working well under bending conditions at both 2.45 GHz and 5.8 GHz. The specific absorption rate (SAR) on 1 g and 10 g of human tissue have also been simulated for the SAR limits to observe the required guidelines by the FCC and ICNIRP. It is also shown from the simulated SAR that the input power of 1 mW obeys the guidelines. In a nutshell, the proposed dual-band semi-flexible antenna is suitable for wearable applications due to its compact size, flexibility in bending conditions regardless of the diameter of human arms and the acceptable SAR limits that obey the FCC and ICNIRP guidelines.

ACKNOWLEDGEMENTS

The authors would like to express their gratitudes to Universiti Tun Hussein Onn Malaysia for the financial assistance in completing this work under the Internal University Grant of Tier 1 (Code No: H247).

REFERENCES

[1] B. Li, & K. W. Leung, "Dielectric-Covered Dual-Slot Antenna for Dual-Band Applications," *IEEE Transactions on Antennas and Propagation*, vol. 55, no. 6, pp. 1768-1773, 2007, doi: 10.1109/TAP.2007.898607.

[2] L. N.-Wu, Lei Zhu, W.-Wa Choi, and Xiao Zhang, "A Low-Profile Aperture-Coupled Microstrip Antenna with Enhanced Bandwidth under Dual Resonance," *IEEE Transactions on Antennas and Propagation*, vol. 65, no. 3, pp. 1055-1062, 2017, doi: 10.1109/TAP.2017.2657486.

[3] V. Gohar, A. Keshtkar, and M. N.-Moghadasi, "Compact and Miniaturized Microstrip Antenna based on Fractal and Metamaterial Loads with Reconfigurable Qualification," *AEU-International Journal of Electronics and Communications*, vol. 83, pp. 213-221, 2018, doi: 10.1016/j.aeue.2017.08.057.

[4] F. Meng, & S. Sharma, "A Single Feed Dual-Band (2.4 GHz/5 GHz) Miniaturized Patch Antenna for Wireless Local Area Network (WLAN) Communications," *Journal of Electromagnetic Waves and Applications*, vol. 30, no. 18, pp. 2390-2401, 2016, doi: 10.1080/09205071.2016.1251854.

[5] P. Xu, M. Li, S. Wang, Y. Zhou, C. Shen, and X. Li, "A Compact Multiband Antenna based on Metamaterial for WLAN/WiMAX/WAVE Applications," *2017 Sixth Asia-Pacific Conference on Antennas and Propagation (APCAP)*, 2017, pp. 1-3, doi: 10.1109/APCAP.2017.8420481.

[6] M. Mantash, S. A. Collardey, C. Tarot, & A. Presse, "Dual-band WiFi and 4G LTE Textile Antenna," *2013 7th European Conference on Antennas and Propagation (EuCAP)*, 2013, pp. 422-425.

[7] R. Avisankar, S. Bhunia, D. Chanda Sarkar, and P. P. Sarkar, "Compact Dual Band Microstrip Antenna Using Square Loop Slot for GSM 1800 and HiperLAN-2 Applications," *Proceedings of the 2nd International Conference on Communication, Devices and Computing*, vol. 602, 2020, pp. 35-43.

[8] Saeed, Saud M., Constantine A. Balanis, Craig R. Birtcher, Ahmet C. Durgun, and Hussein N. Shaman., "Wearable Flexible Reconfigurable Antenna Integrated with Artificial Magnetic Conductor," *IEEE Antennas and Wireless Propagation Letters*, vol. 16, pp. 2396-2399, 2017, doi: 10.1109/LAWP.2017.2720558.

[9] L. Vallozzi, C. Hertleer, & H. Rogier, "Latest Developments in the Field Of Textile Antennas," *Smart Textiles and Their Applications*, pp. 599-626, 2016, doi: 10.1016/B978-0-08-100574-3.00026-6.

[10] J. K. Pakkathillam, & M. Kanagasabai, "Performance Evaluation of a Dual-Band Paper Substrate Wireless Sensor Networks Antenna Over Curvilinear Surfaces," *IET Microwaves, Antennas & Propagation*, vol. 9, no. 8, pp. 715-722, 2015, doi: 10.1049/iet-map.2014.0691.

[11] A. H. Kusuma, A. F. Sheta, I. M. Elshafiey, Z. Siddiqui, Alkanhal, M. A., Aldosari, & S. F. Mahmoud, "A New Low SAR Antenna Structure for Wireless Handset Applications," *Progress in Electromagnetics Research*, vol. 112, pp. 23-40, 2011, doi: 10.2528/PIER10101802.

[12] S. Agneessens, & H. Rogier, "Compact Half Diamond Dual-Band Textile HMSIW On-Body Antenna," *IEEE Transactions on Antennas and Propagation*, vol. 62, no. 5, pp. 2374-2381, 2014, doi: 10.1109/TAP.2014.2308526.

[13] P. M. Rayner, and W. G. Whittow, "Specific Absorption Rate and Efficiency of a Wideband Wearable Monopole Antenna Near the Human Body," *Loughborough Antennas & Propagation Conference (LAPC 2017)*, 2017, pp. 1-5, doi: 10.1049/cp.2017.0234.

[14] K. Zhao, S. Zhang, Z. Ying, T. Bolin, & S. He, "SAR Study of Different MIMO Antenna Designs for LTE Application in Smart Mobile Handsets," *IEEE Transactions on Antennas and Propagation*, vol. 61, no. 6, pp. 3270-3279, 2013, doi: 10.1109/TAP.2013.2250239.

[15] H. M. A. Fahmy, "Wireless Sensor Networks: Concepts, Applications, Experimentation and Analysis," *Springer Singapore*, 2016, doi: 10.1007/978-981-10-0412-4.

[16] G. A. Eyebe, A. Benleulmi, N. Boubekeur, & F. Domingue, "Low-Profile Triband ISM Dipole Antenna," *2016 22nd International Conference on Applied Electromagnetics and Communications (ICECOM)*, 2016, pp. 1-3, doi: 10.1109/ICECom.2016.7843889.

[17] M. Kalyan, and P. P. Sarkar, "Dual Band Compact Monopole Antenna for ISM 2.4/5.8 Frequency Bands with Bluetooth, Wi-Fi and Mobile Applications," *Microwave and Optical Technology Letters*, vol. 59, no. 5, pp. 1061-1065, 2017, doi: 10.1002/mop.30465.
[18] A. I. Hammoodi, H. M. Al-Rizzo, & A. A. Isaac, "A Wearable Dual-Band Square Slot Antenna with Stub for ISM and WiMAX applications," *2015 IEEE International Symposium on Antennas and Propagation & USNC/URSI National Radio Science Meeting*, 2015, pp. 732-733, doi: 10.1109/APS.2015.7304753.
[19] M. A. Osman, M. K. A. Rahim, N. A. Samsuri, & M. E. Ali, "UWB Wearable Textile Antenna," *Jurnal Teknologi*, vol. 58, pp. 39-44, 2012.
[20] S. Singh, R. K. Gangwar, & S. Agarwal, "A Dual-Band T-Shaped Microstrip Antenna for Wearable Application," *International Journal of Electronic and Electrical Engineering*, vol. 7, no. 2, pp. 195-200, 2014.
[21] J., Abd Rahim, M. K., Samsuri, N. A., H. A. M. Salim,, & M. F. Ali, "Embroidered Fully Textile Wearable Antenna For Medical Monitoring Applications," *Progress in Electromagnetics Research*, vol. 117, pp. 321-337, 2011, doi: 10.2528/PIER11041208.
[22] W. Lie, X. Fu, J. He, X. Shi, T. Chen, P. Chen, B. Wang, and H. P eng, "Application Challenges in Fiber and Textile Electronics," *Advanced Materials*, vol. 32, no. 5, Art. no. 1901971, 2019, doi: 10.1002/adma.201901971.
[23] J. Xinghui, M. Zhu, W. Wei, G. Yu, and H. Zho., "A Small-Size and Multi-Band Wearable Antenna with Coplanar Structure," *Journal of Physics: Conference Series*, vol. 1325, no. 1, 2019, Art. no. 012201, 2019.
[24] Balanis, C. A. (Ed.)., "Modern Antenna Handbook," *John Wiley & Sons*, 2011.
[25] P., Ronald, "Dielectric Properties of Biological Materials: Biophysical and Medical Applications," *IEEE Transactions on Electrical Insulation*, vol. El-19, no. 5, pp. 453-474, 1984 , doi: 10.1109/TEI.1984.298769.
[26] Yang, Fan, and Yahya Rahmat-Samii, "Patch Antennas with Switchable Slots (PASS) in Wireless Communications: Concepts, Designs, and Applications," *IEEE Antennas and Propagation Magazine*, vol. 47, no. 2, pp. 13-29, 2005, doi: 10.1109/MAP.2005.1487774.